Oxford Instruments Analytical – **technical briefing**

Energy Dispersive X-ray Microanalysis Hardware

Explained

OXFORD INSTRUMENTS

Introduction

Ease of use has become a major focus in the selection of EDS analyzers. The hardware that acquires the data is often taken for granted.

The detection and measurement of X-rays in an electron microscope requires a complex measurement chain, which, if functioning correctly, can provide the accurate and stable data required to complement the software and allow reliable automatic peak identification and standardless quantitative analysis. The test of a good design is whether results on a given sample remain accurate irrespective of changing count rate or environment.

This guide introduces the operation of the EDS hardware, and highlights the important aspects that make a difference in accurate and efficient X-ray analysis.

X-ray Detector

Pulse Processor

Principal System Components

An EDS system is comprised of three basic components that must be designed to work together to achieve optimum results (Fig. 1).

X-ray Detector

Detects and converts X-rays into electronic signals

Pulse Processor

Measures the electronic signals to determine the energy of each X-ray detected

Analyzer

Displays and interprets the X-ray data

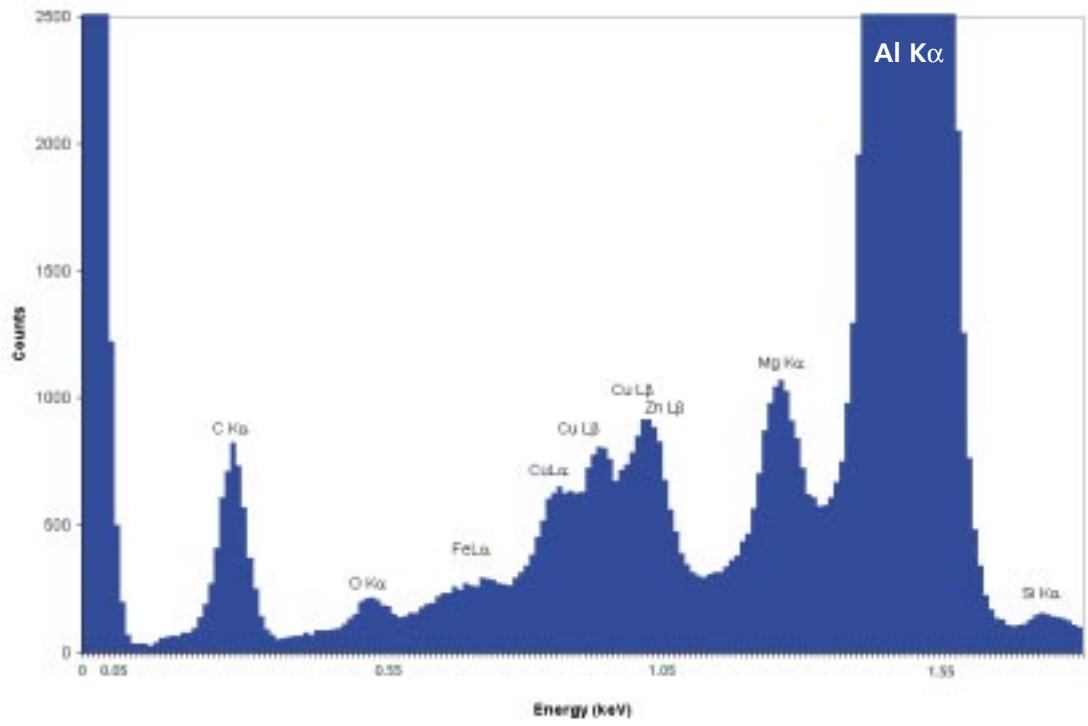

Mg	1.26 +/-	0.05	1.47
Al	89.63 +/-	0.22	94.20
Si	0.26 +/-	0.05	0.27
Mn	0.96 +/-	0.07	0.50
Fe	0.47 +/-	0.07	0.24
Ni	1.44 +/-	0.09	0.69
Cu	3.25 +/-	0.13	1.45
Zn	2.73 +/-	0.14	1.18
Totals	100.00		100.00

Fig. 1.

Analyzer

Components of an EDS Detector

1. Collimator assembly

The collimator provides a limiting aperture through which X-rays must pass to reach the detector. This ensures that only X-rays from the area being excited by the electron beam are detected, and stray X-rays from other parts of the microscope chamber are not included in the analysis.

2. Electron trap

Electrons that penetrate the detector cause background artefacts and also overload the measurement chain. The electron trap is a pair of permanent magnets that strongly deflect any passing electrons. This assembly is only required on detectors with thin polymer windows, as thicker beryllium windows efficiently absorb electrons below 20keV in energy.

3. Window

The window provides a barrier to maintain vacuum within the detector whilst being as transparent as possible to low energy X-rays. There are two main types of window materials. Beryllium (Be) is highly robust, but strongly absorbs low energy X-rays meaning that only elements from sodium (Na) can be detected. Polymer-based thin windows can be made much thinner than Be windows and therefore are transparent to much lower energy X-rays, many allowing detection of X-rays down to 100eV. Although these window materials are far less robust, by placing them on a supporting grid they can withstand the pressure difference between the detector vacuum and a vented microscope chamber at atmospheric pressure. The greater transmission of the polymer-based windows means that they have largely replaced Be as the material used for detector windows.

4. Crystal

The crystal is a semiconductor device that through the process of ionization converts an X-ray of particular energy into electric charge of proportional size. To achieve this a charge-free region within the device is created. Two main materials are used for the detecting crystal. The most common is silicon (Si), into which is drifted lithium (Li) to compensate for small levels of impurity. High purity germanium crystals (HpGe) are also used. Si(Li) was the first material used in EDS detectors and remains the most common choice today. HpGe offers performance advantages when measuring higher energy X-rays.

5. FET

The field effect transistor, normally referred to as the FET, is positioned just behind the detecting crystal. It is the first stage of the amplification process that measures the charge liberated in the crystal by an incident X-ray and converts it to a voltage output.

The EDS Detector

6. Cryostat

The charge signals generated by the detector are small and can only be separated from the electronic noise of the detector if the noise is reduced by cooling the crystal and FET. Most EDS detectors work at close to liquid nitrogen temperatures (90K), and are cooled using a reservoir of liquid nitrogen held in a dewar. The low temperatures required can also be achieved using mechanical cooling devices. However, these are more expensive to build and maintain, particularly if low vibration is essential, and so are normally used only where liquid nitrogen is not available. The 'cold finger' that cools the crystal is insulated from the wall of the detector snout by a vacuum. The vacuum is maintained at a low enough level to prevent the condensation of molecules on the crystal.

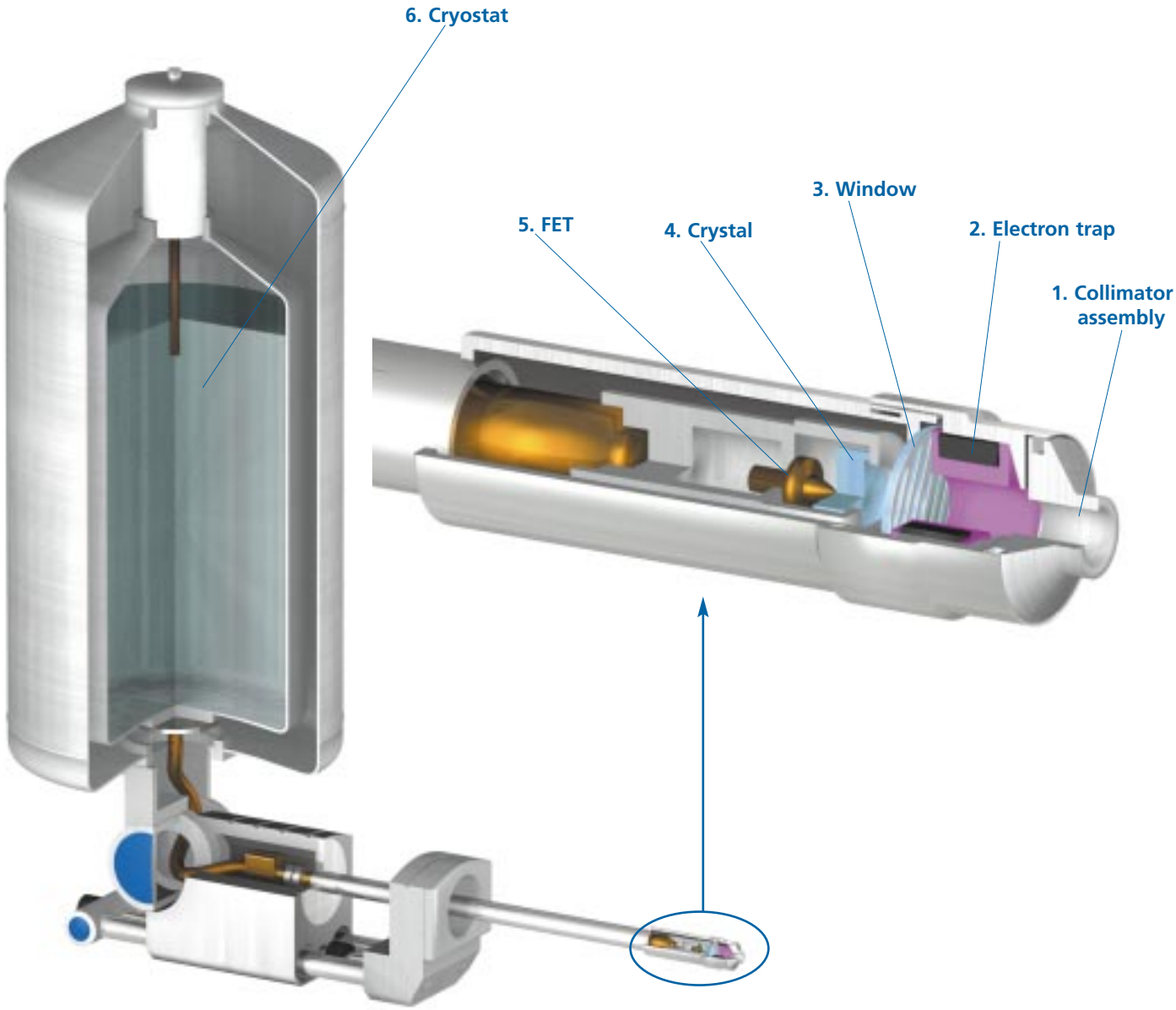

Fig. 2. Cut-away diagram showing the construction of a typical EDS detector.

How the EDS Detector Works

The EDS detector converts the energy of each individual X-ray into a voltage signal of proportional size. This is achieved through a three stage process. Firstly the X-ray is converted into a charge by the ionization of atoms in the semiconductor crystal. Secondly this charge is converted into the voltage signal by the FET preamplifier. Finally the voltage signal is input into the pulse processor for measurement. The output from the preamplifier is a voltage 'ramp' where each X-ray appears as a voltage step on the ramp.

EDS detectors are designed to convert the X-ray energy into the voltage signal as accurately as possible. At the same time electronic noise must be minimized to allow detection of the lowest X-ray energies.

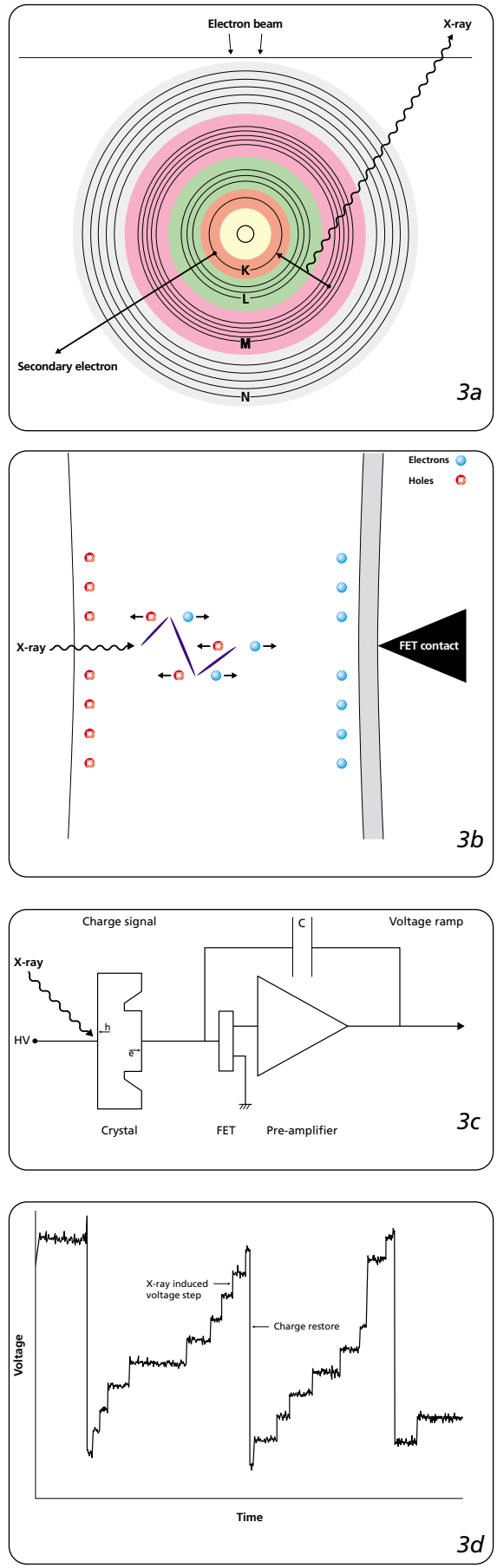

Fig. 3. Conversion of X-ray signals into a voltage 'ramp' by the EDS detector. (a) generation of a characteristic X-ray in a sample by electron bombardment. (b) generation and measurement of electron-hole pairs in the crystal. (c) circuit diagram of the EDS detector. (d) typical output voltage 'ramp' showing events induced by MnKα X-rays.

How the crystal converts X-ray energy into charge

When an incident X-ray strikes the detector crystal its energy is absorbed by a series of ionizations within the semiconductor to create a number of electron-hole pairs (Fig. 3b). The electrons are raised into the conduction band of the semiconductor and are free to move within the crystal lattice. When an electron is raised into the conduction band it leaves behind a 'hole', which behaves like a free positive charge within the crystal. A high bias voltage, applied between electrical contacts on the front face and back of the crystal, then sweeps the electrons and holes to these opposite electrodes, producing a charge signal, the size of which is directly proportional to the energy of the incident X-ray.

The role of the FET

The charge is converted to a voltage signal by the FET preamplifier (Fig. 3c). During operation, charge is built up on the feedback capacitor. There are two sources of this charge, current leakage from the crystal caused by the bias voltage applied between its faces, and the X-ray induced charge that is to be measured. The output from the FET caused by this charge build-up is a steadily increasing voltage 'ramp' due to leakage current, onto which is superimposed sharp steps due to the charge created by each X-ray event (Figs. 3d, 4). This accumulating charge has to be periodically restored to prevent saturation of the preamplifier. Therefore at a pre-determined charge level the capacitor is discharged, a process called restoration. Restoration can be achieved either by pulsed optical restore where light from an LED is shone onto the FET, or by using direct injection of charge into a specially designed FET.

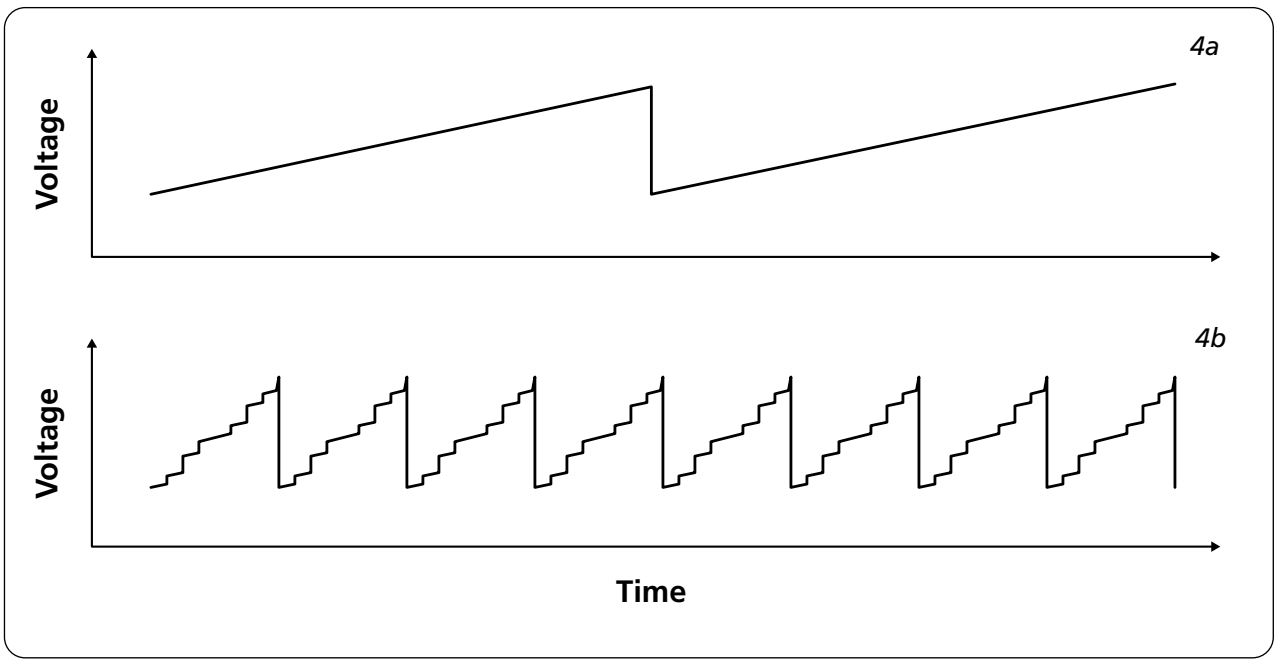

Fig. 4. Output voltage ramp (a) when no X-rays are detected, the ramp results from leakage current from the detector. (b) when X-rays are detected, steps representing each X-ray are superimposed onto the ramp. At high count rates excessive rate of restores can affect the ability of the detector to measure X-rays accurately.

The noise is strongly influenced by the FET, and noise determines the resolution of a detector particularly at low energies. Low noise is also required to distinguish low energy X-rays such as beryllium from noise fluctuations (Fig. 5) . Direct charge restoration via the FET introduces less noise than optical restore. At high count rates, the restoration periods limit the maximum output rate and any after-effects of the restoration (Fig. 4) will affect pulse measurement. Direct charge restoration via the FET is considerably faster and avoids the after-effects associated with optical restore so that noise and resolution are less likely to degrade with increasing count rate.

What Makes a Good X-ray Detector

The following section introduces some of the most important issues that can be used to evaluate the ability of an X-ray detector to accurately and efficiently detect X-rays.

Manganese resolution, MnKα FWHM

Resolution is quoted as the width of the peak at half its maximum height (FWHM). The lower the number the better the resolution a detector has and the better it will be at resolving peaks due to closely spaced X-ray lines.

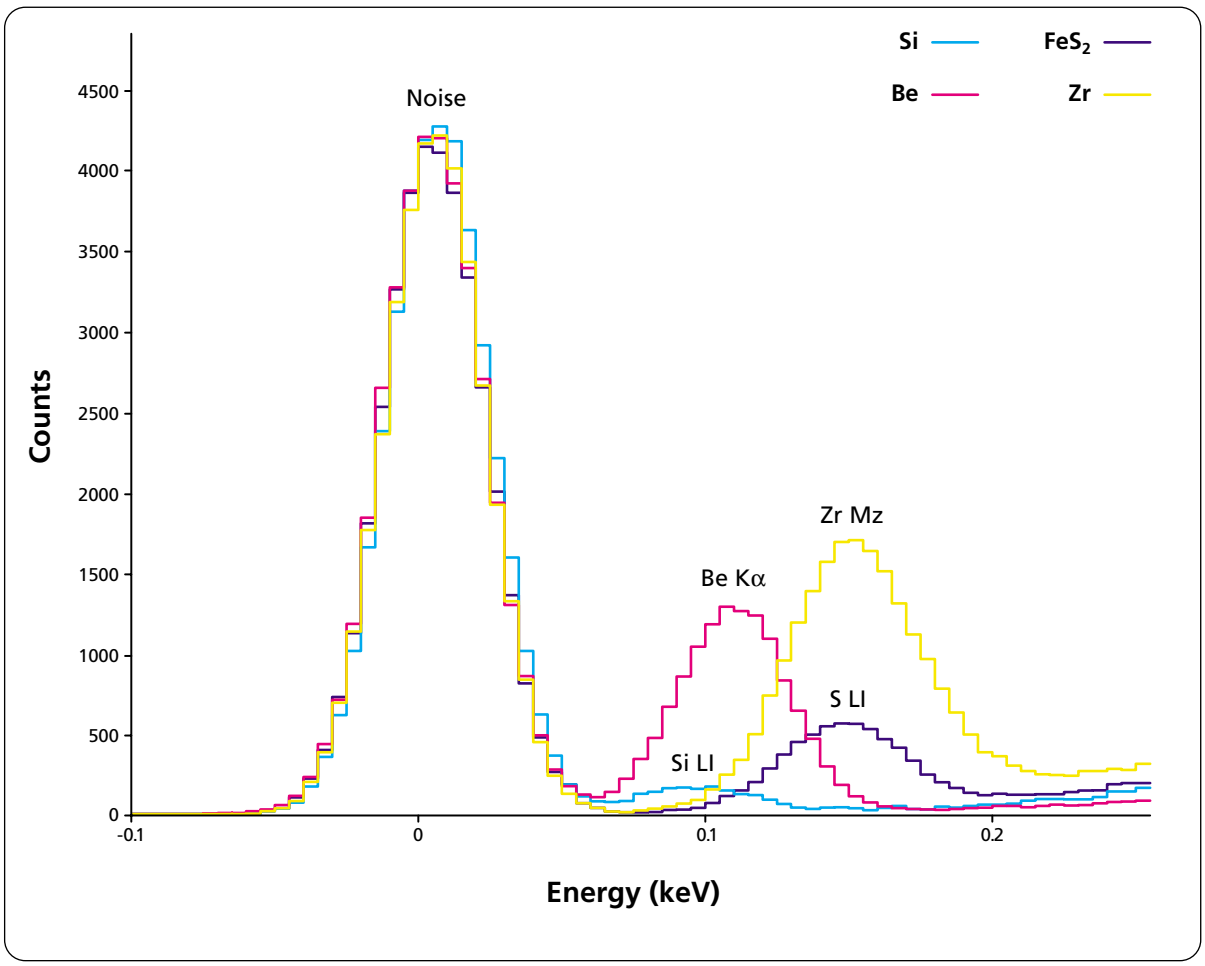

Fig. 5. Spectra collected from Be, Si, FeS_2, and Zr, showing the detection and separation from noise of low energy K, L, and M lines.

Manganese resolution is measured by placing a piece of pure manganese under the electron beam. On a microscope the resolution is often quoted at 1000cps. This count rate is much lower than is used in practice for most microanalysis experiments. It is important to determine whether this resolution is maintained at more realistic and productive count rates.

The importance of low energy resolution

The identification and quantification of closely spaced X-ray peaks becomes easier and more accurate as the separation between them increases. X-ray lines get closer together at low energy and this is apparent in Fig. 6 where the energy of the main alpha line for K, L and M series is plotted for all elements. At the MnKα energy most commonly used to specify EDS resolution, peaks are well separated. However, it is clear that much more serious overlaps occur below 3keV and the resolution performance at low energies is critical to good performance for all elements.

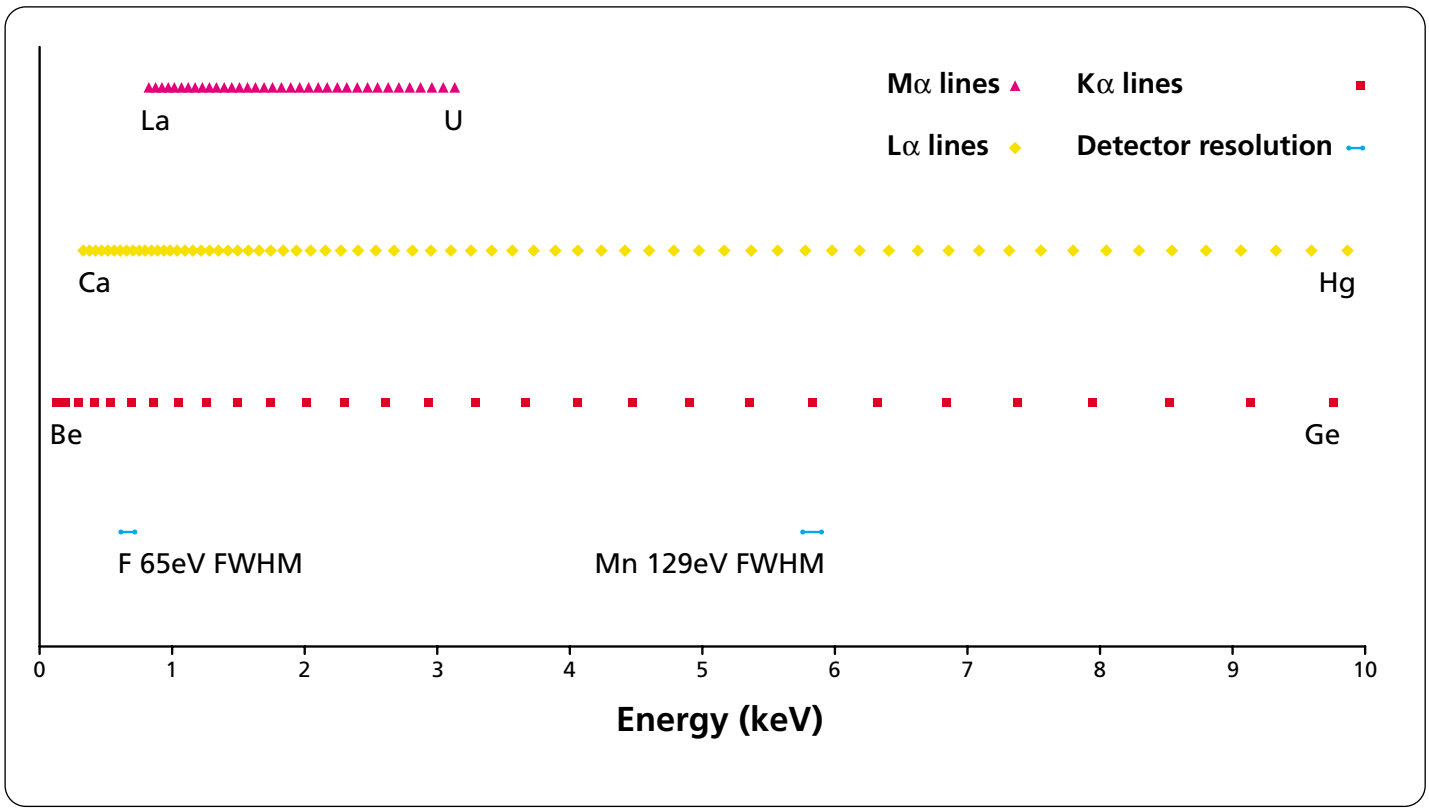

Fig. 6. Energy of Kα, Lα and Mα lines. Note that the separation between lines decreases and density of lines increases at low energy.

When small features <1µm in size are being analyzed, the beam voltage needs to be reduced to avoid electron scattering outside the feature. However, at low kV only low energy lines are available for analysis. Spectra collected from a nickel alloy at 20kV and 5kV (Fig. 7) illustrate the importance of resolution at low energy. When working at 20kV, the separation of widely spaced K lines of Cr, Fe and Ni, will not be affected much by a few eV variation in resolution. When working at 5kV however, where identification relies on L lines, a detector with a few eV better resolution will allow the L lines of Cr, Fe and Ni to be separated enough for confident identification.

Fluorine resolution FKα FWHM

The width of the peaks in a spectrum will vary depending on the energy of the X-ray line. In Fig. 8 this variation with energy has been calculated to show how the resolution should change with X-ray energy for Si(Li) and HpGe detectors with different Mn resolution specifications. The curves are calculated from the equation

$$FWHM^2 = k \cdot E + FWHM_{noise}^2$$

where k is a constant for the detector material, and E is the energy.

These curves demonstrate that as the energy decreases, the resolution of the X-ray peaks improves. The variation is also clearly different for Si(Li) and HpGe crystals. At low energy the electronic noise contribution ($FWHM_{noise}$) has a greater effect on resolution (Fig. 9). Mn FWHM is a very insensitive measure to characterize the noise of a detector and predict the resolution at low energy. Therefore to characterize the resolution of a detector at low energy, the resolution is also quoted for another line, typically fluorine Kα.

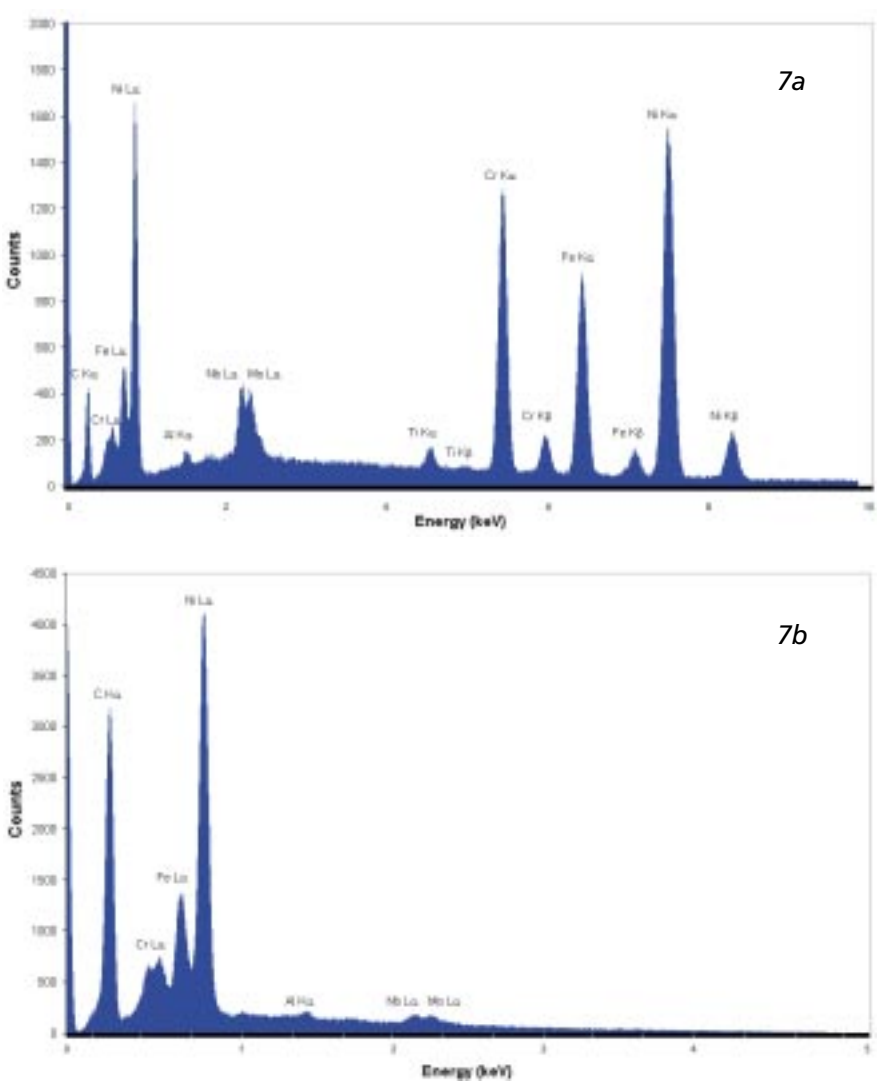

Fig. 7. Spectra collected from a nickel alloy at different accelerating voltages.
(a) 20kV.
(b) 5kV.

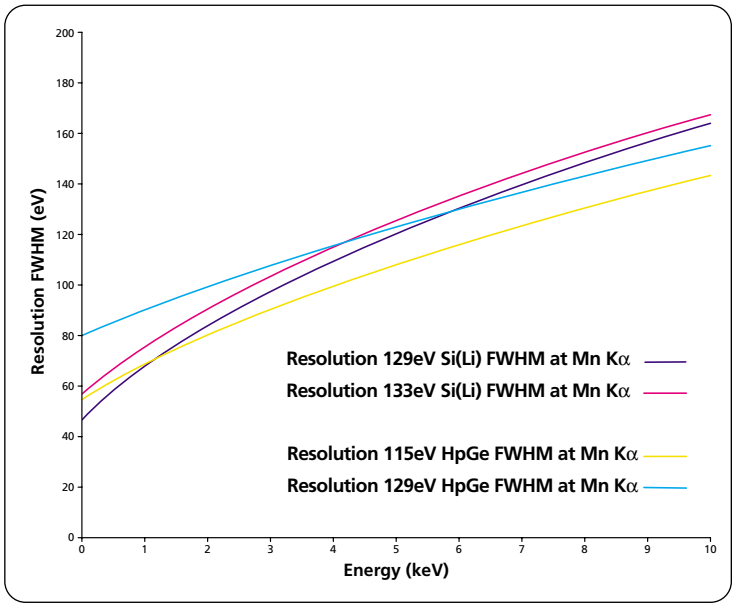

Fig. 8. Curves showing how resolution changes with energy for different detectors. The calculation ignores the effects of incomplete charge collection that can make some detectors give worse performance than these curves predict, particularly at low energies.

Incomplete charge collection

If all the electron-hole pairs generated by an X-ray are not swept to the electrical contacts, the charge signal measured by the FET will be lower than expected, and the energy measured lower than the energy of the incident X-ray. This phenomenon is known as incomplete charge collection (ICC), and results in counts appearing in the spectrum at lower energies than the energy of the X-ray which they represent, typically as a tail on the low energy side of the peak. All detectors suffer from incomplete charge collection to some extent. Low energy X-rays have a very shallow depth of penetration and ICC is usually poor near the front contact. The peak for a low energy X-ray will therefore be broader and have a mean energy lower than expected, due to varying levels of charge collection as each X-ray is measured (Fig. 9).

Thus, incomplete charge collection results in detectors with resolutions measured at low energy that are worse than those predicted by theory. In extreme cases it can be the dominant factor controlling resolution at these very low energies (Fig. 9).

Carbon resolution CKα FWHM

It is more important to know what the resolution specification of a detector is at low energy than it is at MnKα. A detector with good energy resolution at low energy will have good resolution throughout the X-ray spectrum. The same is not true in reverse. A good manganese specification guarantees nothing about performance at low energy. This is because a measurement of resolution at low energy is affected by both noise and incomplete charge collection.

The resolution of the CKα peak measured using pure carbon is very useful due to its sensitivity to incomplete charge collection. A low value guaranteed here really does mean excellent detector resolution for all energies.

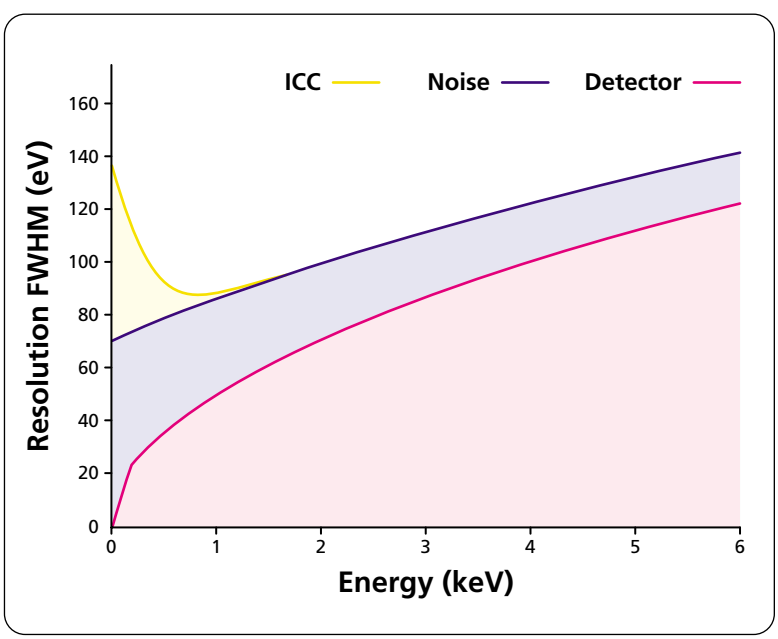

Fig. 9. The variation in detector resolution with energy is controlled by the contribution of three factors: a constant dispersion based on the crystal material used in a detector, the level of electronic noise, and low energy peak broadening due to incomplete charge collection. The curves here are based on a detector with a resolution of 140eV at manganese that has severe incomplete charge collection.

Detector specifications based on tests using an Fe^{55} radioactive source

Testing the performance of an EDS detector using a radioactive source is convenient for a detector manufacturer because it can be done without having to mount a detector on an electron microscope column. However, Fe^{55} source specifications don't necessarily guarantee the performance when mounted on a column and collecting X-rays emitted during electron bombardment. They are also limited in scope and do not reveal some important aspects of detector performance, in the real situation of electron microscope-based X-ray microanalysis.

The reason that the resolution of a detector is traditionally specified for Manganese Kα X-rays at 5.895 keV, is because this is the energy of the most intense X-ray line emitted by the Fe^{55} source (Fig. 10).

One useful feature of the Fe^{55} source is the absence of the continuum or bremsstrahlung X-rays that would be generated in an electron microscope. Therefore, in an Fe^{55} spectrum the very low intensity background at lower energies than the characteristic Mn X-ray peaks is due to incomplete charge collection. The most common measurement of ICC is the peak: background ratio comparing the height of the MnKα peak to the average background between 0.9-1.1keV (Fig. 10). Events appearing at 1keV correspond to MnKα photons where 83% of the charge has not been collected, whereas events appearing at say 4keV have lost 32% of the charge. Although the original IEEE standard suggested measurement at several energies, manufacturers have most commonly used 1keV. As shown in Fig. 10, 1keV is typically the lowest part of the ICC background and a low value at this energy (high peak:background ratio) does not

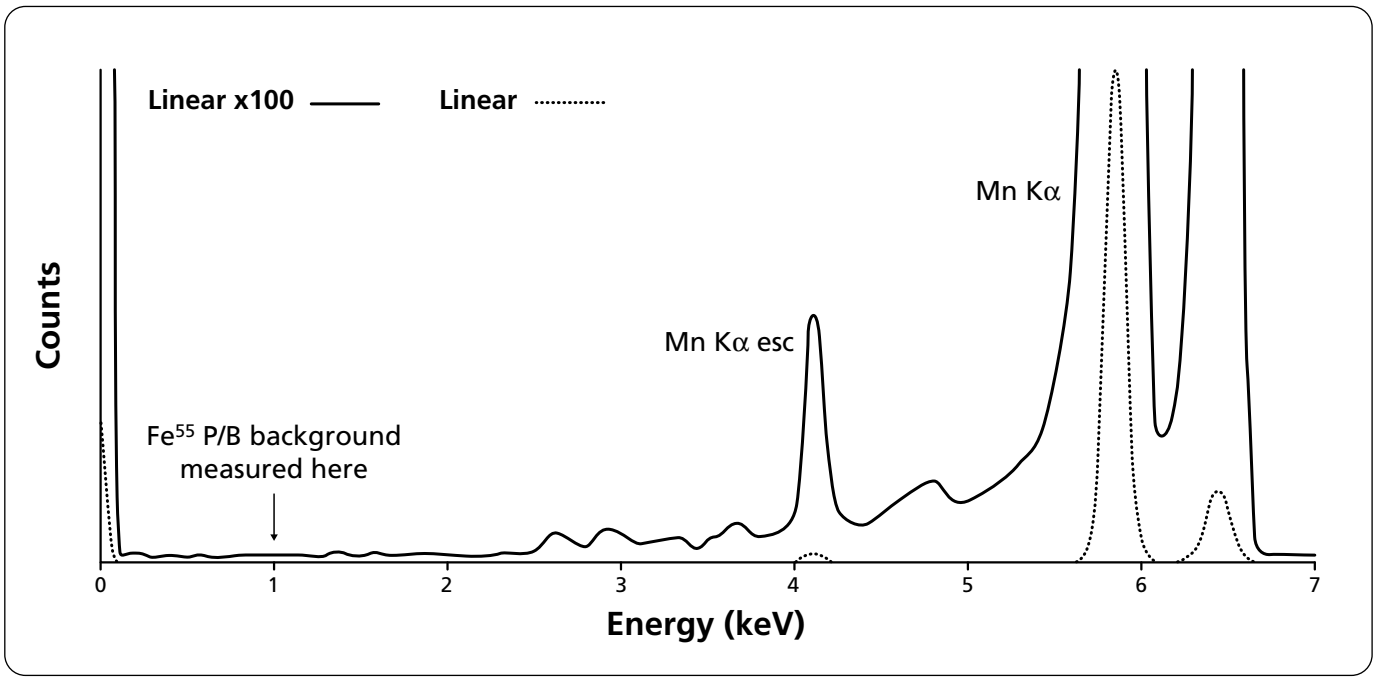

Fig 10. A schematic of a spectrum collected from an Fe^{55} radioactive source showing how peak:background ratio is measured on the bench.

guarantee that charge collection will be good for the smaller charge losses that contribute to the tail or plateau on the low energy side of a peak. Fe^{55} peak:background only gives a general indication of charge collection efficiency, but does not ensure good peak shapes or give any indication of ICC for low energy X-rays. Incomplete charge collection is most important where X-rays are strongly absorbed and only penetrate a short distance into the crystal, for example just above the absorption edge of the elements making up the crystal (1.84keV for Si(Li) detectors), and for very low energy X-rays (less than 0.5keV). The CKα resolution measurement on the microscope represents a more useful and sensitive measurement of incomplete charge collection than peak:background ratios measured with an Fe^{55} source. Low values for CKα FWHM guarantee excellent charge collection, and good peak shapes at all energies.

Detector performance changes with time

A major cause of detector degradation over time is the build up of contaminants that absorb X-rays before they can be detected by the crystal. Common examples include the condensation of oil on the collimator or detector window and ice forming on the face of the crystal. These contaminants will cause preferential absorption and a drop-off in sensitivity for low energy X-rays.

Ice forms on the cold crystal due to the migration and condensation of any water molecules in the detector vacuum.

Two sources of water vapor exist: impurities present during manufacture, and molecules that migrate through the window when the detector is exposed to high vapor pressures. Modern manufacturing techniques mean that when installed, a detector vacuum should be free of water molecules. In SEMs where variable vacuum or environmental modes are used, the detector spends time in conditions where water is present in the microscope chamber. Some types of polymer thin window, which are predominant in modern EDS detectors, have been shown to degrade and become porous under conditions where water molecules are present.

A gradual decrease in low energy sensitivity over time will result in a decrease in the height of peaks at low energy. This can be checked by monitoring the relative height of K and L lines from a transition metal element. The ratio of L to K line heights from pure nickel measured at 20kV is a common test used. A more sensitive test for the presence of ice on a crystal is to look at the L spectrum from pure Cr. The L line spectrum consists of the Ll line at 0.5keV, and the Lα line at 0.571keV. The Lα line is on the high energy side of the oxygen absorption edge (energy 0.531keV) whilst the Ll line is on the low energy side. Therefore CrLα X-rays are much more efficiently absorbed by ice than CrLl X-rays. On a detector with little or no ice on the crystal face the Lα line should be higher than the Ll line (Fig. 11b). On a detector which has ice built up on the crystal the Ll line will be higher (Fig. 11a).

The ice must be removed to regain the light element sensitivity of a detector. This can be done in two ways. If the detector is thermally cyclable it can be allowed to warm up. When the crystal starts to warm the ice will sublime and the vapor will disperse into the vacuum. When the detector is cooled down again the water vapor will normally condense within the dewar because this area cools down first.

This technique is time-consuming, requiring the liquid nitrogen reservoir in the dewar to be exhausted which can take a number of days, or to speed up the process, the detector can be removed from the column and the nitrogen poured out. Some detectors have a built-in heating circuit called a conditioner. This circuit warms up the crystal enough to sublime off any ice. Conditioning can be done whilst the detector is cooled down on the microscope column, and can remove any ice in as little as 2 hours.

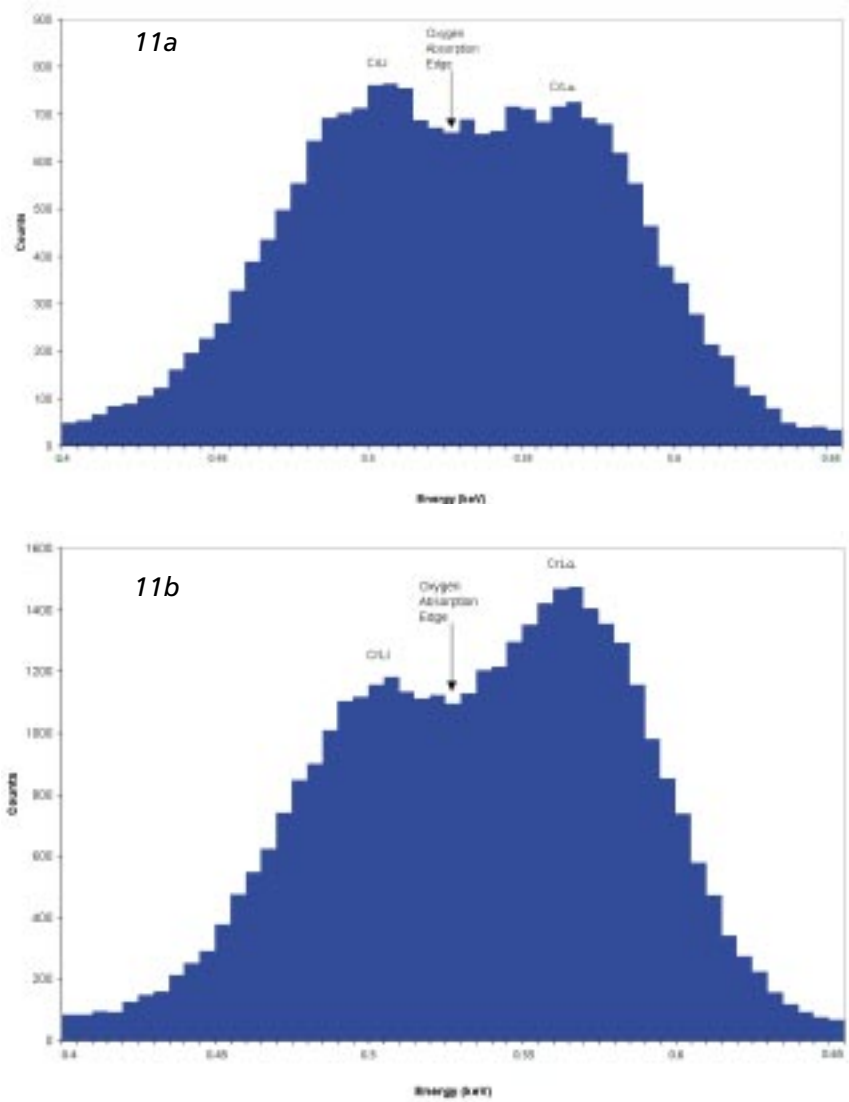

Fig. 11. CrL spectra collected from pure Cr at 5kV. (a) A spectrum collected from a detector used on a variable vacuum microscope showing CrLα absorption equivalent to 100nm of ice. (b) A spectrum collected from the same detector after the ice layer has been sublimed away by a two hour conditioning cycle.
Note partially resolved CrLl and Lα lines and their relative intensities.

Geometry

To a first approximation, X-rays are emitted equally in all directions, therefore the collection efficiency is governed by the proportion of space intercepted by the detector active area (A). This in turn is proportional to the 'solid angle' which would be 2π steradians if all the X-rays in a hemisphere above the specimen were collected. If d is the sample-crystal distance, then solid angle = A/d^2 is a useful approximation for solid angles less than 0.2 steradians.

EDS detectors are available with different sizes of crystals. The crystal size is often measured in area, $5mm^2$, $10mm^2$, $30mm^2$, $50mm^2$ etc. There is a trade off in performance; normally the larger the crystal, the worse will be its resolution, particularly at low energy.

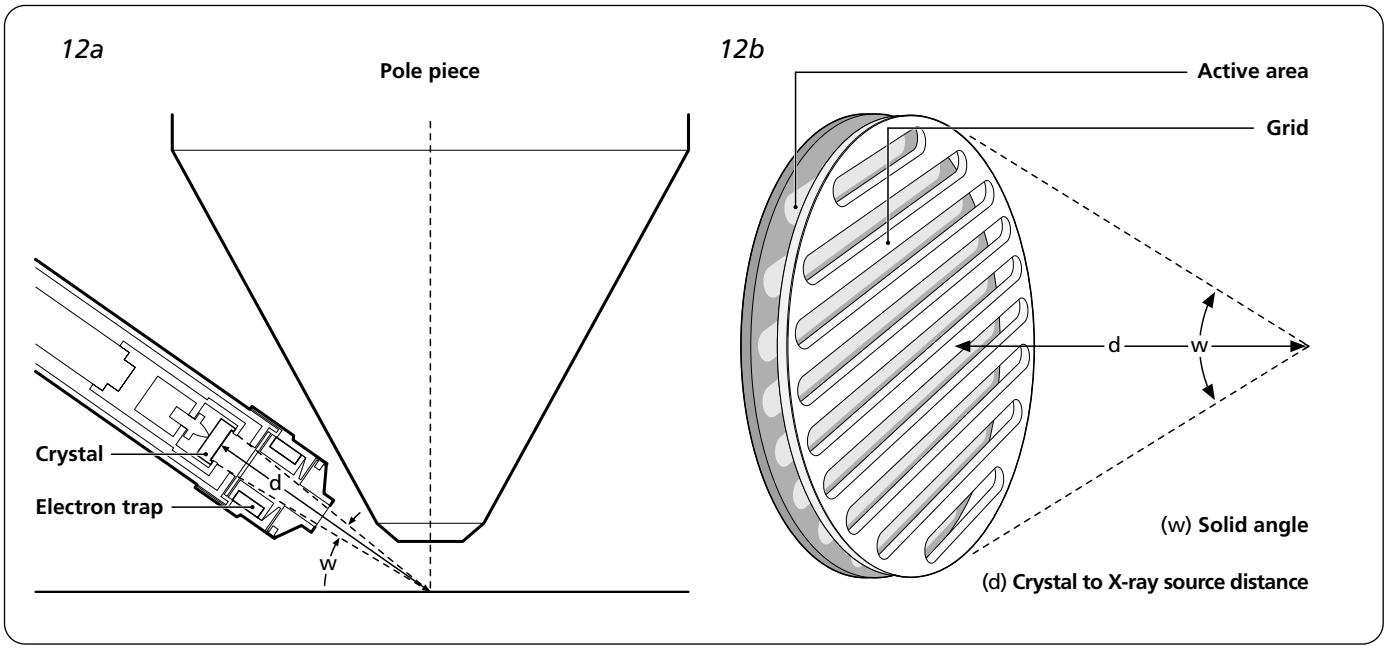

Fig. 12. Calculation of the solid angle of an EDS detector. (a) The detector size and the geometry of the microscope control the distance between X-ray source and crystal. (b) The solid angle is proportional to the active area of the crystal, rather than its actual area, and inversely proportional to the square of the distance.

The collection efficiency is more sensitive to the distance between crystal and the sample, and for maximum efficiency the detector must be positioned as close to the sample as possible. A 10mm^2 crystal at a distance of 5cm will have the same solid angle as a 30mm^2 crystal at 8.7cm. The distance the crystal will be from the source of X-rays on the sample will depend on the dimensions and design of the detector and also the geometry of the microscope (Fig. 12a). The type of collimator and window assemblies used also affect the solid angle.

The requirement for an electron trap places the crystal further from the sample (Fig. 12a), and the need for a support grid for the window reduces the active area A by typically 20% compared to self-supporting thin windows (Fig. 12b).

Therefore if count rate is an issue, when considering crystal size it is much more useful to know what the maximum solid angle will be on the microscope to be used, rather than just the crystal area. For most microscopes sufficient solid angle can be achieved with 10mm^2. In some situations, for example when using a transmission electron microscope, the X-ray signal is very low, and a bigger crystal is used to improve signal collection.

Summary

- **The EDS detector converts the energy of a single X-ray photon into a step of proportional size on a voltage ramp using a semiconductor crystal and FET-preamplifier**
- **Good analytical performance requires good resolution at low energies**
- **Mn resolution (5.9keV) does not give a reliable indication of resolution at low energies because it is insensitive to ICC and does not separate noise and detector material components**
- **F resolution (0.7keV) is more sensitive to low energy noise and is a better guide to low energy performance**
- **C resolution accounts for noise and is very sensitive to incomplete charge collection. An excellent resolution at carbon implies good resolution at all energies**
- **The collection efficiency of X-rays is determined by the collection solid angle, not the area of the crystal**

Section 2: The Pulse Processor

The Role of the Pulse Processor

The charge liberated by an individual X-ray photon appears at the output of the preamplifier as a voltage step on a linearly increasing voltage ramp (Fig. 13a). The fundamental job of the pulse processor is to accurately measure the energy of the incoming X-ray, and give it a digital number that is used to add a count to the corresponding channel in the computer (Fig. 13c). It must also optimize the removal of noise present on the original X-ray signal. It needs to recognize quickly and accurately a wide range of energies of X-ray events from 110eV up to 80keV. It also needs to differentiate between events arriving in the detector very close together in time, otherwise the combination produces the spectrum artefact called pulse pile-up.

Signal measurement

There are a number of ways of measuring the size of the steps on the voltage ramp, which depend on the type of pulse shaping being used: digital or analog.

Analog pulse shaping

In analog shaping the signal from the preamplifier is converted to a pulse by way of analog shaping electronics (Fig. 14). The height of the pulse is then measured and converted into a digital signal by an analog to digital converter (ADC). A longer peaking time (T_P) is used to reduce noise and improve resolution.

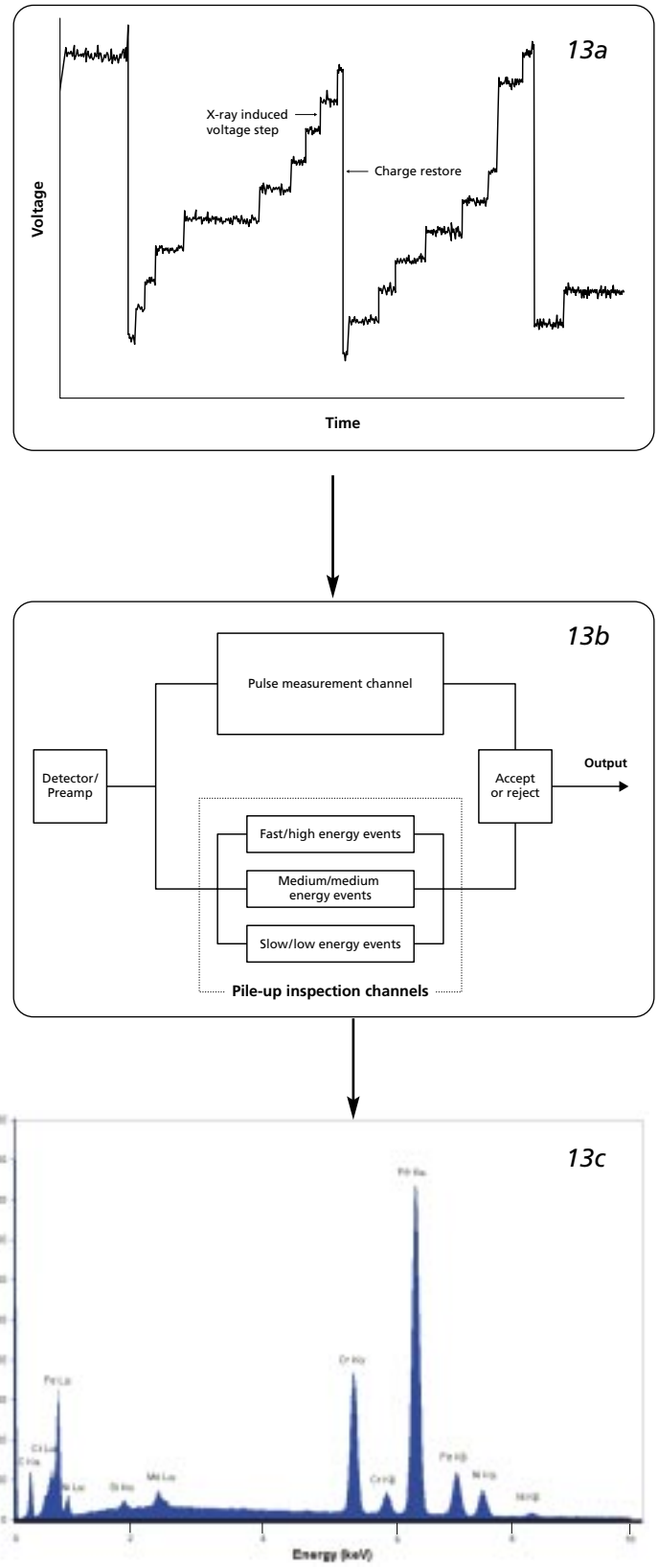

Fig. 13. Accurate measurement of the voltage ramp is the role of the pulse processor.
(a) typical output voltage ramp showing events induced by MnKα X-rays.
(b) layout of a typical pulse processor showing the measurement and pulse pile-up inspector channels.
(c) Output of the measured steps gives an X-ray spectrum showing number of counts vs. energy.

Accurate height measurement of each pulse requires the shaping circuitry to be reset to the baseline level before another event can be accepted for measurement. The decay time (T_D) gives the effective minimum time before another step can be measured accurately (Fig. 14).

The challenge with analog shaping is to compensate for changes in the baseline. To measure a 10keV photon to within 1eV requires the baseline to be known within 0.01% of the pulse height. The time required for the pulse to decay to below 0.01% of the pulse height will be many times the peaking time. As the count rate increases the residuals on the baseline left over from each shaped pulse begin to build up, resulting in a measurable shift in the apparent baseline. In addition, the baseline will move at high input rates due to the cumulative after-effects of all the large restore signals. Thus, as the input count rate increases, peaks will shift in position.

Even at low count rates, the slope on the voltage ramp will affect the position of the baseline. This slope, caused by leakage current from the detector (see Fig. 4), will mean that shaped pulses will not return exactly to zero, and therefore the baseline always has some offset.

When calibrating systems with analog shaping two key adjustments are required. One to compensate for detector leakage current, another to compensate for count rate-induced peak shift. Since the degree of shift depends on the shaping time, these adjustments have to be performed for every shaping time constant and gain setting. Count rate effects may also vary with spectrum content and even if exact compensation is achieved for an 'average' sample spectrum, peak shifts of a few eV may still be expected when different samples are analyzed. Furthermore, if detector leakage changes, the calibration process for baseline offset has to be repeated.

Some pulse processors are described as digital, because they use digital circuits and software instead of control knobs to control the circuitry. These processors will have the same problems with baseline measurement and calibration shown by any pulse processor that uses analog shaping.

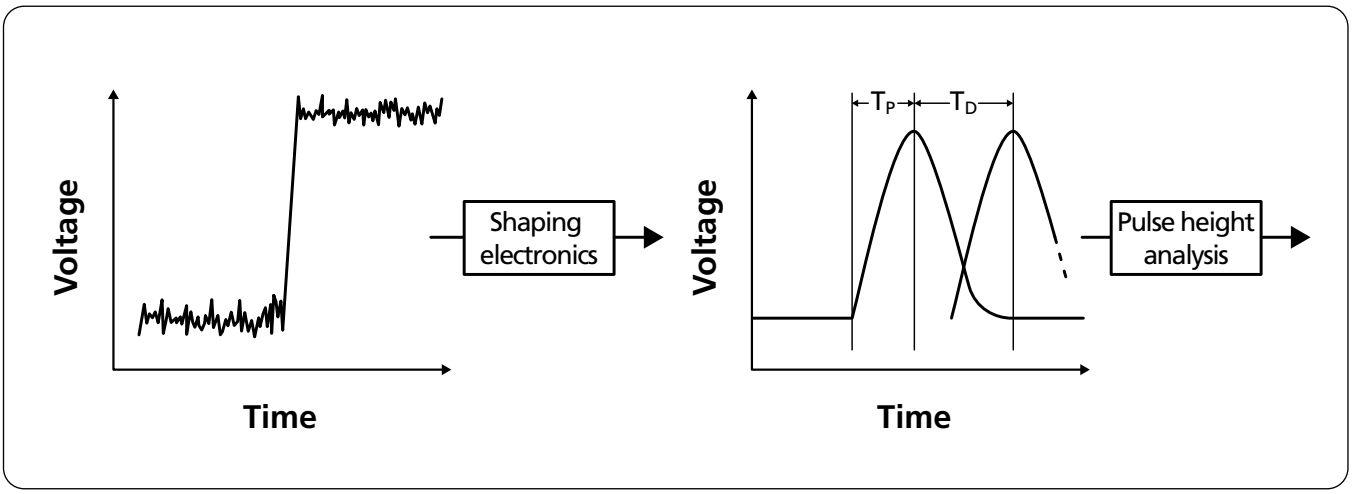

Fig. 14. Measurement of a step on the voltage ramp by analog shaping electronics. Each pulse is shaped for a peaking time T_P to remove noise, and to form a pulse that can be measured by a pulse height analyzer. T_D is the time taken for the pulse to decay sufficiently close to zero to allow another pulse to be measured accurately.

Time variant shaping

Time variant shaping can be used to overcome the calibration problems and rate sensitivity of analog shaping (Kandiah et al. 1975). By switching to a very short time constant right after the measurement is complete, the pulse returns very rapidly to the baseline. The shaping circuit can then be switched back to long time constants ready to measure the next voltage step. This method removes any count rate-induced shift but requires complex circuitry because each event has to be recognized as being present before the sequence of shaping can be initiated. In the absence of any real events, the electronics can also measure the voltage ramp, and therefore monitor the baseline automatically, so that changes in the slope of the ramp caused by variable detector leakage are compensated and peak shift is negligible.

Digital pulse shaping

In a processor using digital shaping, the signal from the preamplifier is digitized at the input of the pulse processor, and shaping and noise reduction are achieved by digital computation.

The preamplifier output is sampled continuously by an analog to digital converter (ADC) and X-ray pulse heights are measured by subtracting the average of one set of values, measured before an X-ray event, from that for another set, measured after the event. The resultant value of the step measurement is then sent directly to the computer multichannel analyzer.

The noise on the voltage ramp from the detector is effectively filtered out by averaging the signal (Fig. 15). The time over which the waveform is averaged (often called the process time) is equivalent to the peaking time for an analog shaper (T_P).

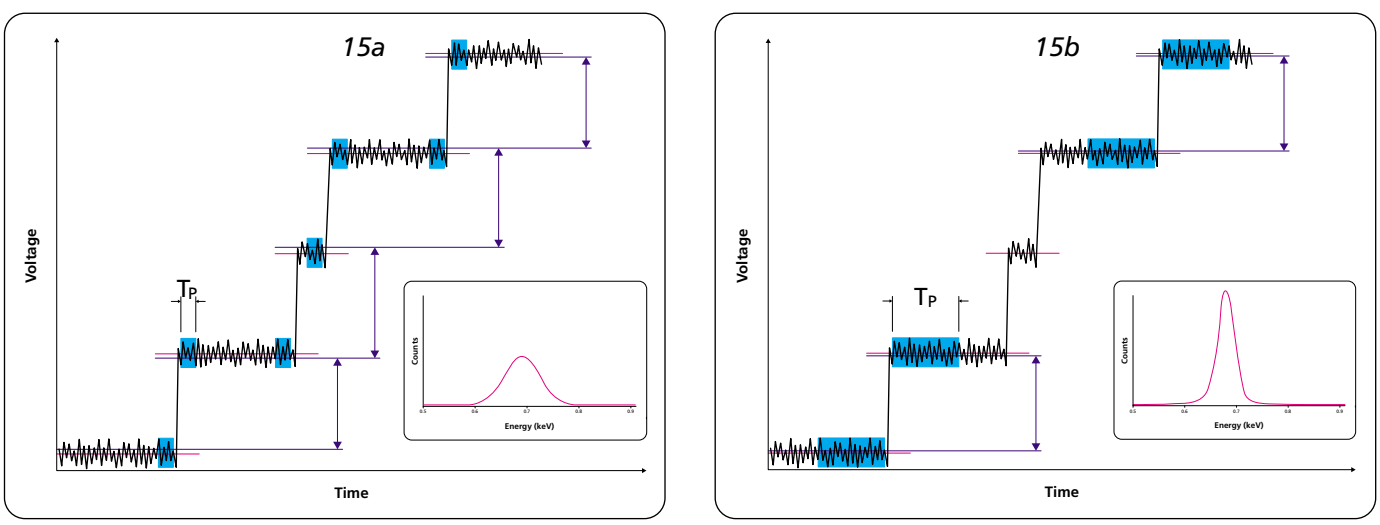

Fig. 15. Measurement of steps on a voltage ramp by averaging differing numbers of measurements of the signal. (a) Short T_P permits all steps to be measured, but the variation of each measured step is large, so the X-ray energy is not measured accurately and peaks show poor resolution. (b) Long T_P means that some steps arrive too close together to be measured. However, noise averaging is better and therefore peaks show better resolution.

By measuring the voltage ramp in this way the benefits of perfect baseline recovery are achieved without the complexities required for time variant shaping circuits. Therefore peaks should not shift with count rate. There is also the potential for measuring the zero baseline ('strobing') by averaging the digital output of the ramp when no events are present (Fig. 18a). This will provide not only automatic correction for changes in the slope of the voltage ramp caused by changes in detector leakage current, but will also measure the effective noise resolution. Calibration procedures for processors using digital pulse shaping should be straightforward and reliable. One energy calibration should be sufficient to guarantee accurate energy calibration at all count rates.

Processors with fixed process time

The longer the process time (T_P), the lower the noise. If noise is minimized, the resolution of the peak displayed in the spectrum is improved (see Fig. 15), and it becomes easier to separate or resolve, from another peak that is close in energy (Fig. 16). However, there is a trade-off between the process time that is used, and the speed at which data can be measured. The longer the process time, the more time is spent measuring each X-ray, and the fewer events that can be measured. The longest process time used by a processor gives the best resolution possible while the shortest process time gives the maximum throughput into the spectrum, but with the worst resolution (Fig. 16).

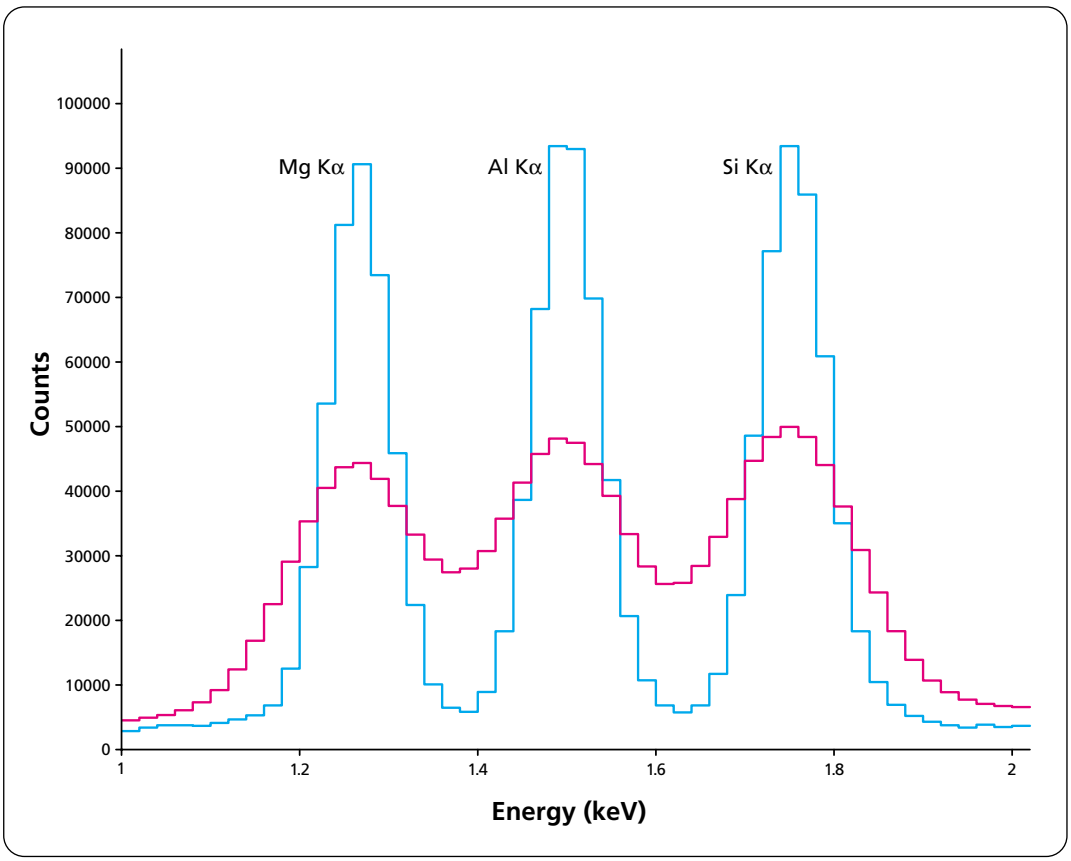

Fig. 16. Spectra collected at short (red) and long (blue) process times.

Productivity depends on the rate of counts measured, called the acquisition rate, rather than the input rate (into the detector).
As the input rate increases so will the acquisition rate, but an increasing number of events are rejected because they arrive in a shorter time period than T_P (Fig. 15). If input rates increase sufficiently, the proportion rejected will exceed the increase in measured events and the acquisition rate will start to decrease with further increases in input rate (Fig. 17).

Therefore for each process time there is a maximum acquisition rate (Fig. 17) which corresponds to the maximum speed possible for a chosen resolution. The maximum acquisition rate for each process time is characteristic of the pulse processor used. By determining, for each processor setting, the maximum acquisition rate and the resolution at this rate, the productivity and performance of a processor can be evaluated.

In a processor where the process time is fixed, the trade off between resolution and acquisition rate can be controlled and the resolution accurately defined.

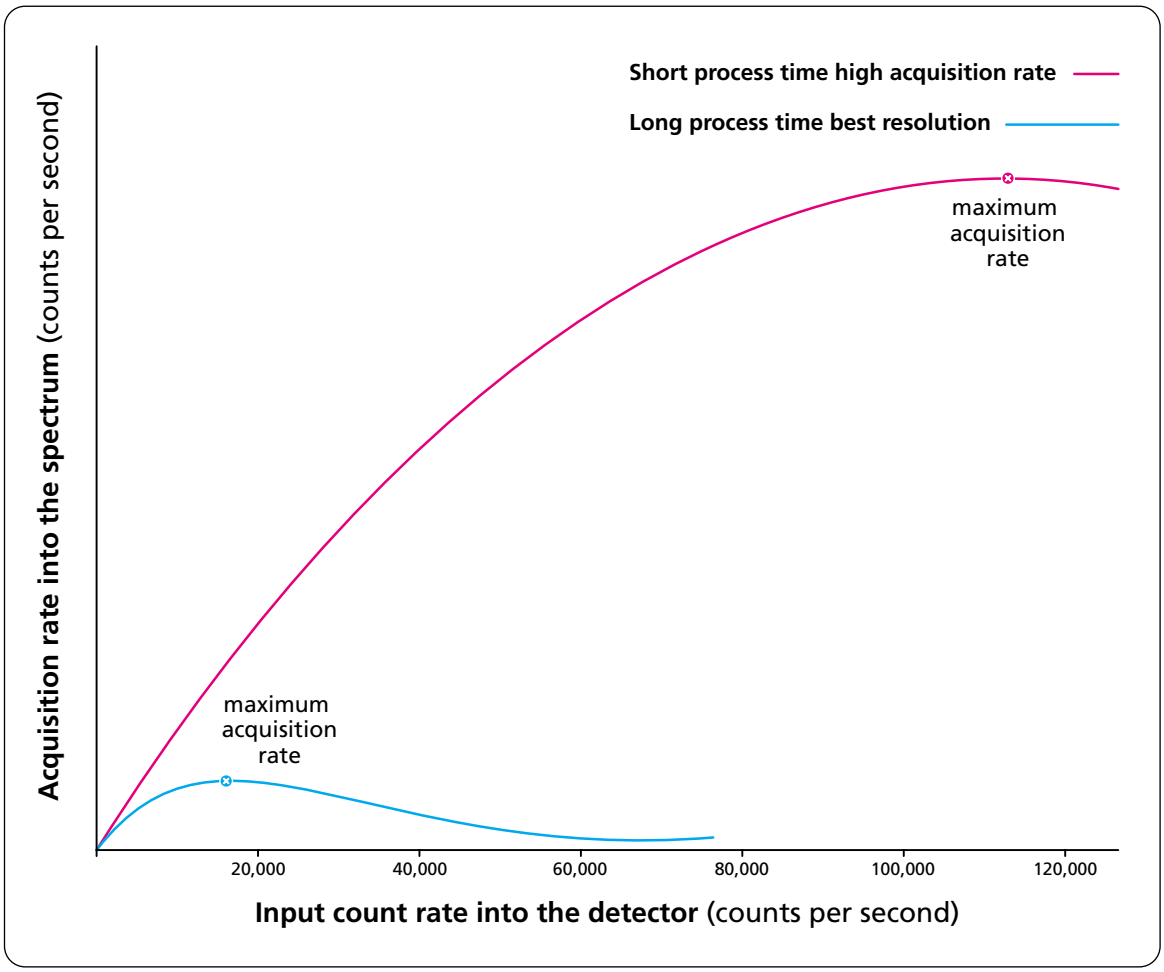

Fig. 17. Curves showing the variation of acquisition rate with input rate for two fixed process times. The longer process time gives good resolution but limited maximum acquisition rate, the short process time allows much higher acquisition rates but resolution is worse.

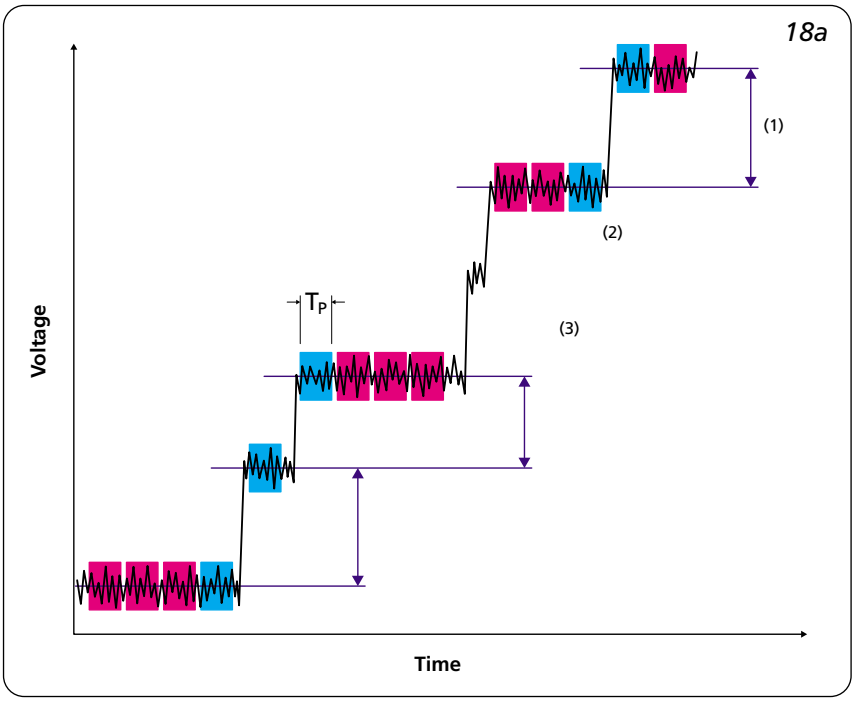

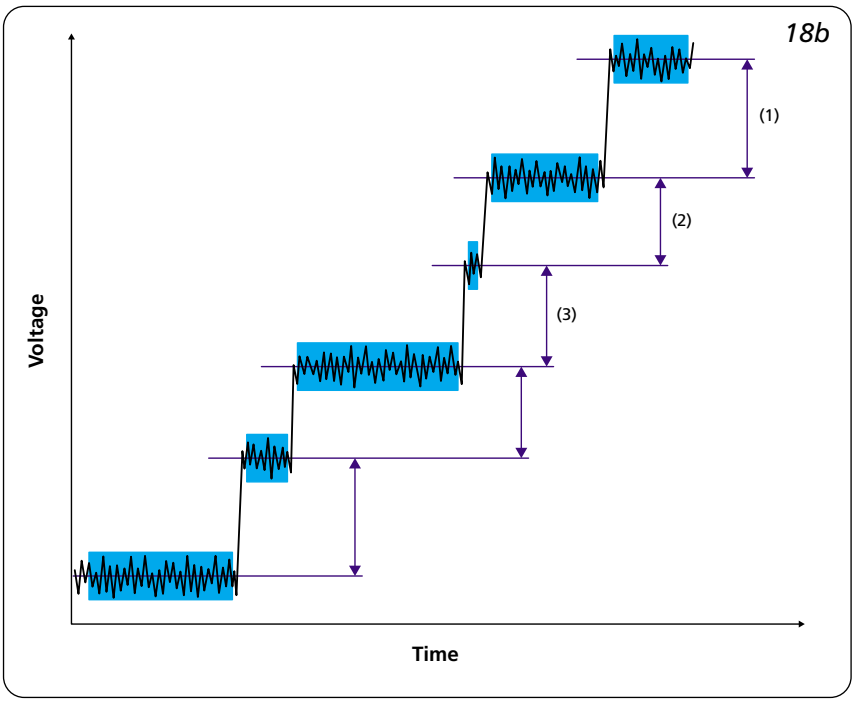

Fig. 18. Voltage ramps measured by:
(a) a digital pulse processor with a fixed process time, and
(b) a digital pulse processor using adaptive pulse shaping.
The blue areas show the averages used to measure each step. With a fixed process time, events like (2) and (3) which arrive closer together than T_P are rejected. The fixed process time electronics continuously 'strobes' the zero level (red areas) when not measuring the voltage steps. In the adaptive pulse shaper the averaging time is allowed to vary before and after the step. Therefore some events like (1) are measured with longer averaging time than with the fixed shaper but others like (2) and (3) are measured with short averaging times and therefore worse resolution. The effective noise contribution is a complex mixture of Gaussians of different width and there is no way of measuring equivalent noise resolution by 'strobing'. Throughput is therefore better than with a fixed shaper but resolution and peak shape change with count rate and resolution cannot be predicted by strobe measurement.

Processors which use adaptive pulse shaping

It is possible to use variable averaging times to measure the size of each step. Events that arrive far apart can be measured with more noise averaging than events arriving close together (Fig. 18b). This produces a spectrum where each peak is built up of many Gaussian shapes with a distribution of resolutions determined by the distribution of the timing of the arrival of events on the voltage ramp.

At low input rates this type of processor will deliver similar resolution to a fixed processor using a long process time. However, as the input rate is increased the adaptive shaper begins to use shorter averaging times and the resolution becomes worse, although the acquisition rate is better than with a fixed process time. The adaptive pulse shaper thus ensures efficient measurement of as many X-rays as possible. The maximum acquisition rate that this type of processor can achieve will still be controlled by the shortest time allowed to measure a voltage step. This will be similar to the maximum count rate achieved by a fixed process time processor using its shortest process time.

Using this type of shaping the analyst loses control over resolution of the spectrum. The resolution varies with count rate, for example when moving from one phase to another, or with any change in beam current. 'Strobing' cannot be used to measure resolution because the averaging time is variable. As a consequence resolution and peak shape are poorly defined and this compromizes the accuracy of spectrum processing.

Does resolution change with count rate?

Even when using a fixed process time resolution may change with count rate when using analog or digital shaping. For example, this may be due to changes in the slope of the ramp caused by variable leakage current, or where the contribution of after-effects of ramp restore increases with restore rate. Furthermore, instabilities in the detector and variations in electronic baseline may be accentuated by increasing count rate.

Although most systems should be able to maintain resolution sufficiently for X-ray mapping, only the best designs will achieve stability (within 1%) required for accurate peak deconvolution.

Pulse pile-up inspection

Pulse pile-up inspection channels are used to ensure that only one photon is measured at a time.

Inspection circuits (Fig. 13b) sense the arrival of an incoming event. Each circuit has a time constant that determines the smallest voltage step and therefore the lowest energy event that can be inspected. If the time constant is too short, noise levels will be high and low energy events will not be efficiently detected, but if too long it will be unable to distinguish between closely arriving events and the pile-up protection efficiency of the circuit will be compromized. Pulse processors should have more than one of these circuits, each with a different time constant to ensure efficient pulse pile-up protection over the full range of detectable energies. This means the processor will be suitable for use with a thin polymer window detector for light element detection, as well as for measuring higher energy lines.

The result of efficient pulse inspection is to provide a spectrum with no pile-up artefacts such as sum peaks. These peaks, caused when two X-rays arriving close together are counted as one, may cause incorrect peak identification, and inaccurate results (Fig. 19). If a photon is missed by all the inspection channels, it can contribute to a tail or 'pile-up continuum' on the high side of every peak.

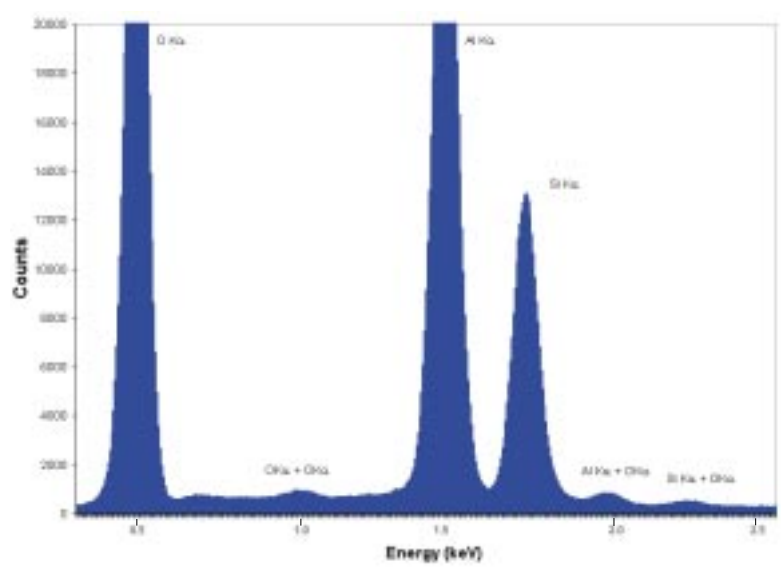

Fig. 19. A spectrum collected from kyanite (Al_3SiO_5) at high input rate, shows sum peaks that could suggest the presence of elements not present in the sample. The peak at 1keV is the result of oxygen X-rays arriving together (O + O sum peak), but may be confused for a NaKα peak. The Al + O sum peak at about 2keV may be incorrectly identified as PKα.

Comparing Different Pulse Processors

For accurate and efficient EDS analysis the performance of the pulse processor is as important as the detector.

EDS detector specifications typically reveal the best possible performance that the detector can achieve. Any pulse processor will perform its best at very low count rates, when the voltage steps on the ramp are widely spaced and easy to measure. Therefore detector specifications are often quoted at 1000cps. However, this count rate is well below what is required for efficient analysis and only the best designs of pulse processor will maintain good and stable detector performance as the input count rate is varied.

How does performance change when the count rate is increased? At more commonly used input rates between 2000 and 10000cps, processors may not be able to maintain the best resolution if resolution degrades with count rate, or process time is shortened to achieve a useful acquisition rate. Therefore one useful measure of how an EDS hardware system will perform is the resolution achieved when the input rate is at least 2500cps, and the acquisition rate is below the maximum for the process time chosen.

Modern EDS software is designed to give reliable automatic identification of X-ray peaks and accurate standardless analysis. This is a relatively straightforward task when peaks are well separated, but for overlapped peaks where there is no clear valley between the peaks, accurate energy calibration is vital. Some systems may appear to have stable performance with count rate because peaks do not move more than 5eV and X-ray line markers are always in the correct channel at 10eV/channel. However, when quantifying peaks about 35eV apart (e.g. SiKα and WMα) only a 4eV shift in energy calibration can introduce a 10 weight% error (Statham 2002). If the resolution also varies and the width of peaks is wrongly predicted by the software then larger errors may occur.

Analog pulse shaping designs have difficulty maintaining a stable baseline so the energy calibration may vary as count rate increases. Time variant shapers or digital pulse shapers should show much less variation, and provide more reliable results, without the need to keep input rate constant. Moreover, processors which are able to constantly monitor the zero level will be able to measure shifts in the baseline and, in addition, some systems can also monitor resolution changes for correction by software.

The best method to test how energy calibrations and resolutions change over a useful operating count rate range, and how well these changes are compensated, is to analyze real samples at a useful range of input rates, for example 1000, 2500, 5000 and 10000cps. By doing this the effect of any variation on the ability of a system to perform reliable analysis can be tested. The ability to resolve a severe overlap can be tested by analyzing a pure material for elements known not to be present. For example, by collecting spectra from a pure element such as Si, at different count rates.

If the spectra are quantified assuming Si, and Ta and W are present (TaM and WM are very close to SiK), a system that will provide accurate analysis in this count rate range should find levels of Ta and W below statistical significance at all count rates. By overlaying spectra collected at the different rates it may also be possible to see peak shifts or resolution changes with count rate.

For example Fig. 20 shows four spectra collected from pure silicon at different input rates using a digital pulse processor where count rate stability is good. Quantitative analysis of these spectra, assuming Si, Ta and W are present (Table 1) shows that within statistical significance only Si is present, whatever count rate is used to collect the data.

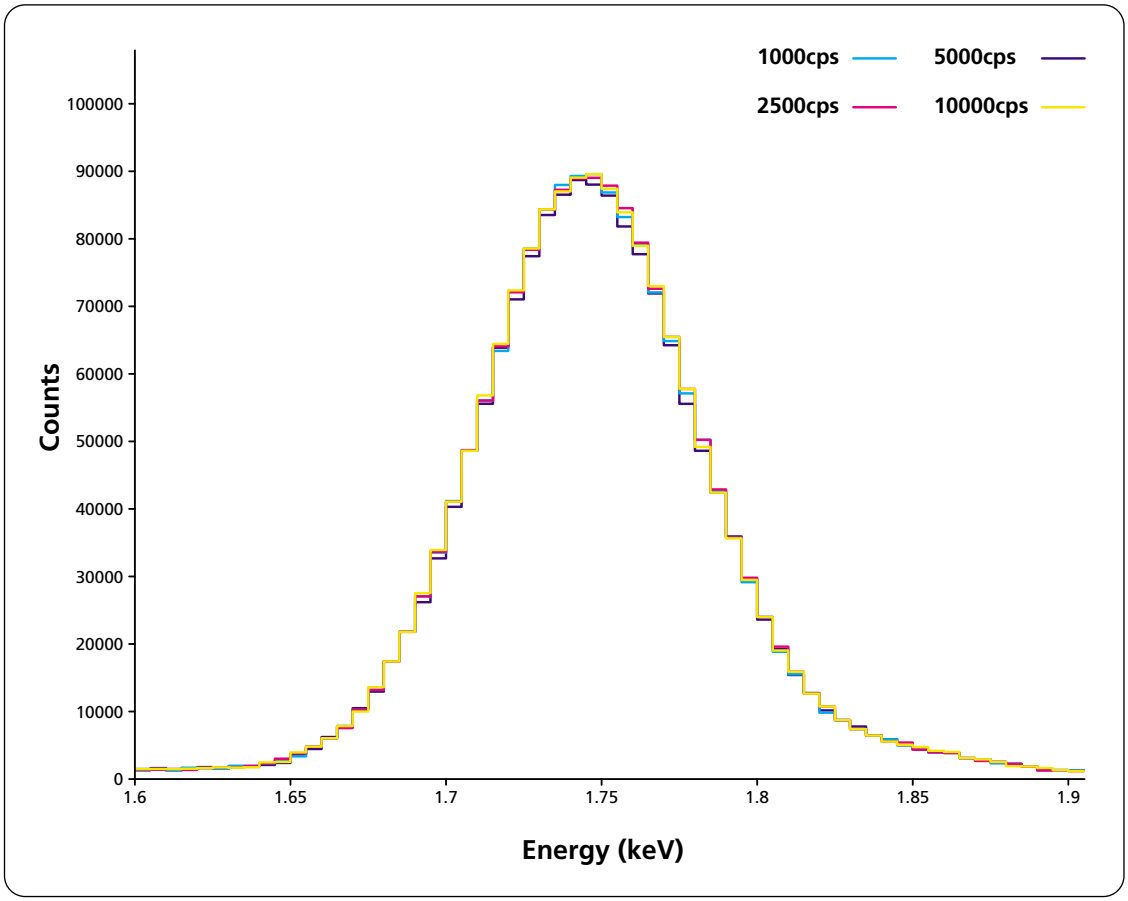

Fig. 20. Spectra collected from pure silicon at 1000, 2500, 5000 and 10000 cps input rate using a digital pulse processor measuring at the same process time. Even when displayed at 5eV per channel no change in resolution or position can be seen for these four spectra.

	1000cps	2500cps	15000cps	10,000cps
Si	99.68 ± 1.78	99.43 ± 1.41	99.90 ± 0.97	99.23 ± 0.90
Ta	-0.82 ± 1.56	0.31 ± 1.22	-0.99 ± 0.85	0.04 ± 0.78
W	1.14 ± 0.89	0.26 ± 0.70	1.09 ± 0.49	0.74 ± 0.46

Table 1
Quantitative analysis of pure silicon calculated from the spectra shown in Fig 20 assuming Si, Ta and W are present. At all input rates Ta and W are below statistical significance (3 sigma). Note that negative numbers should be reported, because negative values greater than statistical significance also indicate incorrect spectrum deconvolution.

Summary

- **Both detector and pulse processor are equally important parts of the measurement chain**
- **Pulse processor performance is characterized by the maximum acquisition rate and resolution achievable at each process time**
- **Measuring the change in energy calibration and resolution as the count rate changes shows how reliably the measurement chain will provide accurate data for automatic peak identification and standardless quantitative analysis**
- **Even small changes in resolution or energy calibration can lead to large errors when analyzing severely overlapped X-ray lines**

References

K. Kandiah, A. J. Smith and G. White, IEEE Trans. Nucl. Sci., NS-22, 2058 (1975)

P.J. Statham, In Proceedings NIST-MAS Special Topics Workshop, "Understanding the Accuracy Barrier in Quantitative Electron Probe Microanalysis and the Role of Standards" NIST, Gaithersburg, MD, USA, April 8-11, (2002)

Oxford Instruments Analytical

UK
Halifax Road, High Wycombe
Bucks, HP12 3SE England
Tel: +44 (0) 1494 442255
Fax: +44 (0) 1494 461033
Email: analytical@oxinst.co.uk

Australia
Sydney, N.S.W. 1715
Tel: +61 2 9484 6108
Fax: +61 2 9484 1667
Email: sales@oxinst.com.au

Austria
A – 1030 Wien
Tel: +43 (0) 1 710 61 98
Fax: +43 (0) 1 710 61 98
Email: rob.wills@oxinst.at

China
Beijing
Tel: +86 (0) 10 6833 0336/5/4
Fax: +86 (0) 10 6833 0337
Email: oiadmin@oxford-instruments.com.cn

France
Saclay, Cedex
Tel: +33 (0) 1 69 85 25 24
Fax: +33 (0) 1 69 41 86 80
Email: analytical-info@oxford-instruments.fr

Germany
Wiesbaden
Tel: +49 (0) 6122 937 176
Fax: +49 (0) 6122 937 178
Email: analytical@oxford.de

Japan
Tokyo
Tel: +81 (0) 3 5245 3591
Fax: +81 (0) 3 5245 4466/4477
Email: yasunori.yoda@oxinst.co.jp

Latin America
Clearwater FL
Tel: +1 727 538 7702
Fax +1 727 538 4205
Email: oxford@gate.net

Scandinavia
Link Nordiska AB
Lidingö, Sweden
Tel: +46 8 590 725 50
Fax: +46 8 590 725 58
Email: info@linknord.se
Web: www.linknord.se

Singapore
Tel: +65 6337 6848
Fax: +65 6337 6286
Email:
analytical.sales@oxford-instruments.com.sg

USA
Concord MA
Tel: +1 978 369 9933
Toll Free: +1 800 447 4717
Fax: +1 978 369 8287
Email: info@ma.oxinst.com

www.oxford-instruments.com

Ref: OIA/074/A/0702

PATENTS
EP 0325383
EP 0302716
US 4931650
GB 2192091
US 5170229
US 5357110
JP 2557692
JP 2581597
EU 0568351

BSI REGISTERED
UKAS QUALITY MANAGEMENT 003
CERTIFICATE NUMBER FM29142

OXFORD INSTRUMENTS